JPE 18-6-3

https://doi.org/10.6113/JPE.2018.18.6.1634
ISSN(Print): 1598-2092 / ISSN(Online): 2093-4718

Deadbeat Direct Active and Reactive Power Control of Three-phase PWM AC/DC Converters

Ali Gandomkar* and Jul-Ki Seok†

†,*Power Conversion Laboratory, Dept. of Electrical Engineering, Yeungnam University, Gyeongsan, Korea

Abstract

This study focuses on a high-performance direct active and reactive power controller design that is successfully applicable to three-phase pulse width modulation (PWM) AC/DC converters used in renewable distributed energy generation systems. The proposed controller can overcome the sluggish transient dynamic response of conventional controllers to rapid power command changes. Desired active and reactive powers can be thoroughly obtained at the end of each PWM period through a deadbeat solution. The proposed controller achieves an exact nonlinear cross-coupling decoupling of system power without using a predefined switching table or bang/bang hysteresis control. A graphical and analytical analysis that naturally leads to a control voltage vector selection is provided to confirm the finding. The proposed control strategy is evaluated on a 3 kW PWM AC/DC converter in the simulation and experiment.

Key words: Deadbeat (DB) solution, Direct active and reactive power controller (DPQC), Nonlinear cross-coupling decoupling, Three-phase PWM AC/DC converter

I. INTRODUCTION

The renewable distributed energy generation technology integrated into microgrids is continuously being developed to meet future energy demands. Future distributed energy systems will deploy additional DC architectures along with the improvement of the DC power technology because of the reliability, power quality, and easy integration of different types of power sources resulting from the minimal requirements for power conversion stages. However, such an approach may be prone to issues such as instantaneous perturbation in the integration of power consumption and power regeneration, which can result in grid instability or outages. Power regulation with fast and accurate dynamic responses is vital to cope with these essential issues [1]-[3]. The slow dynamic responses of power control may result in the uncontrollability of the DC side voltage.

Theoretically, renewable distributed energy systems generally require AC/DC conversion stages to draw power from (renewable) AC power sources or power systems, converting AC to DC with fast dynamic responses and smart power flow management. Among all the AC/DC conversion topologies, pulse width modulation (PWM) AC/DC converters have received considerable attention in the field of high-performance applications due to their outstanding features, such as high efficiency, bidirectional power flow capability, sinusoidal input currents with adjustable power factors, and wide output voltage range [4]. One important issue relevant to the control of PWM AC/DC converters is their transient response to abrupt changes in dynamic loads or instantaneous control commands with their sensitivity to non-ideal supply voltages. Their sluggish transient characteristics, such as slow command tracking in transient regions, may periodically impose uncontrollability of the DC bus voltage and power [5], [6].

Given their expansive applications in a variety of industrial environments, different control strategies have been introduced according to their performance improvement over the last decades [5]-[13].

Proportional integral (PI) or hysteresis band/look-up table-based controllers [7] are mainly embedded in early control techniques, such as voltage-oriented control [8] and direct power control (DPC) techniques [9]. In hysteresis band/look-up table-based controllers, the utilization of a finite number of voltage vectors results in large power ripples and

Manuscript received Mar. 29, 2018; accepted Aug. 29, 2018
Recommended for publication by Associate Editor Hongfei Wu.
†Corresponding Author: doljk@ynu.ac.kr
Tel: +82-53-810-2484, Fax: +82-53-810-4767,Yeungnam University
*Power Convers. Lab., Dept. of Electrical Eng., Yeungnam Univ., Korea

variable switching frequencies during a single control period. An add-on control solution is required due to the slow transient responses of integral actions to dynamic load changes in PI-type controllers [10]. Various embodiments of model predictive control (MPC) [11]-[13] are recently emerging as promising control techniques to achieve fast transient responses. However, with MPC, several complex cost functions must be predetermined under different operating regions to achieve optimal performance.

Another way to optimize digital control dynamic responses and their performance is through the well-known deadbeat (DB) controller [14], [15]. In [14], an MPC-based DB direct power controller was proposed to achieve considerable steady-state performance improvement; however, this controller still requires switching vector selection, and it cannot directly couple the nonlinear cross-coupling between active and reactive powers. DB control was employed for current mode regulations of active power filters in [15]. However, the fastest transient current dynamics do not necessarily guarantee the fastest transient power dynamics because current control leaves active/reactive powers in an open-loop state.

The current work presents a direct active and reactive power controller (DPQC) in the discrete-time domain that is applicable to three-phase PWM AC/DC converters. The main idea implies the use of DB-DPQC for constant PWM switching frequencies. The proposed scheme inherently decouples the nonlinear cross-coupling between active power and reactive power without any voltage vector selection process or cost functions. In addition, the proposed technique secures the power regulation at every sampling instant with regard to the accessible converter voltage, which provides the fast, stable, and non-oscillatory transient dynamic responses over wide power operating ranges and a constant DC link voltage. This study reports a graphical and analytical analysis that naturally leads to a control voltage vector selection within the hexagonal voltage limits, thereby supporting the hypothesis. Comprehensive collections of simulations and experiments are conducted to evaluate the feasibility of the proposed control scheme.

II. General Principles of DB-DPQC Algorithm

A. Dynamic System Model

Fig. 1 shows the circuit diagram of a three-phase two-level PWM AC/DC converter. The AC side voltage in the d-q synchronous reference frame is described as follows:

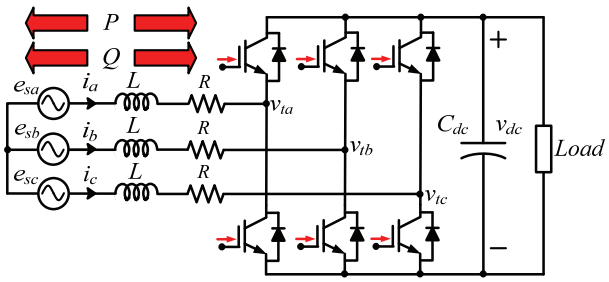

Fig. 1. Circuit diagram of three-phase PWM voltage source converter.

$$\begin{cases} \dfrac{di_d(t)}{dt} = \dfrac{1}{L}e_{sd}(t) - \dfrac{R}{L}i_d(t) - \dfrac{1}{L}v_{td}(t) + \omega i_q(t) \\ \dfrac{di_q(t)}{dt} = \dfrac{1}{L}e_{sq}(t) - \dfrac{R}{L}i_q(t) - \dfrac{1}{L}v_{tq}(t) - \omega i_d(t) \end{cases}, \quad (1)$$

where $\mathbf{e}_{sd,q}$, $\mathbf{i}_{d,q}$, and $\mathbf{v}_{td,q}$ represent the d-q components of the three-phase grid voltage (e_{sa}, e_{sb}, and e_{sc}), three-phase current (i_a, i_b, and i_c), and converter terminal voltage (v_{ta}, v_{tb}, and v_{tc}), respectively. The angular frequency of the grid voltage is assigned as ω, the inductance L is the boost inductor, and R stands for its equivalent series resistance. If the selected switching period (T_s) is sufficiently small, then the substitution of differential operators in (1) results in algebraic equations with a first-order discrete Euler approximation over one T_s as follows:

$$\begin{cases} \dfrac{i_d(k+1)-i_d(k)}{T_s} = \dfrac{1}{L}e_{sd}(k) - \dfrac{R}{L}i_d(k) - \dfrac{1}{L}v_{td}(k) + \omega i_q(k) \\ \dfrac{i_q(k+1)-i_q(k)}{T_s} = \dfrac{1}{L}e_{sq}(k) - \dfrac{R}{L}i_q(k) - \dfrac{1}{L}v_{tq}(k) - \omega i_d(k) \end{cases}. \quad (2)$$

B. Power Control Model

The application of instantaneous active and reactive power theory, namely, p_{ins} and q_{ins}, to the three-phase converter, can be expressed as

$$p_{ins}(t) = \frac{3}{2}\left(e_{sd}(t)i_d(t) + e_{sq}(t)i_q(t)\right), \quad (3)$$

$$q_{ins}(t) = \frac{3}{2}\left(e_{sq}(t)i_d(t) - e_{sd}(t)i_q(t)\right). \quad (4)$$

From (3) and (4), deriving difference equations in discrete time as (5) and (6) is possible.

The rate of grid voltage changes can be imperceptible over T_s in a discrete-time system with a latched voltage input. This rate can be approximated as

$$\frac{p_{ins}(k+1)-p_{ins}(k)}{T_s} = \frac{3}{2}\left(\frac{e_{sd}(k+1)-e_{sd}(k)}{T_s}i_d(k) + e_{sd}(k)\frac{i_d(k+1)-i_d(k)}{T_s} + \frac{e_{sq}(k+1)-e_{sq}(k)}{T_s}i_q(k) + e_{sq}(k)\frac{i_q(k+1)-i_q(k)}{T_s}\right), \quad (5)$$

$$\frac{q_{ins}(k+1)-q_{ins}(k)}{T_s} = \frac{3}{2}\left(\frac{e_{sq}(k+1)-e_{sq}(k)}{T_s}i_d(k) + e_{sq}(k)\frac{i_d(k+1)-i_d(k)}{T_s} - \frac{e_{sd}(k+1)-e_{sd}(k)}{T_s}i_q(k) - e_{sd}(k)\frac{i_q(k+1)-i_q(k)}{T_s}\right). \quad (6)$$

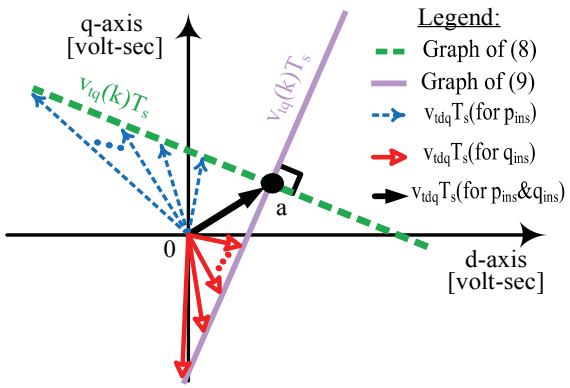

Fig. 2. Corresponding voltage–second lines, their relevant voltage vectors, and the intersection point of two lines on the d-q plane.

$$\begin{cases} e_{sd}(k+1) \cong e_{sd}(k) \\ e_{sq}(k+1) \cong e_{sq}(k) \end{cases}. \tag{7}$$

Integrating (2) and (7) into (5) and (6) forms familiar straight line equations of Y = MX + B and Y = M'X + B' on the complex d-q plane as (8) and (9), respectively.

Fig. 2 shows the plot of each line in the d-q voltage–second plane. According to (8) or (9), some infinite possible input voltage vectors (see dashed blue and red color vectors) can realize the desired changes in either active or reactive power over the next sample time instant(s). With two different command conditions, choosing a voltage vector to satisfy active and reactive powers simultaneously is impossible. Among all voltage vectors, only one voltage vector ensures the active and reactive power magnitudes if two lines intersect at one point "a". Notably, two lines are always orthogonal to each other on the complex d-q plane, as shown in Fig. 2.

The voltage vector drawn from the origin to the intersection point of "a", which is scaled by T_s, is applied to find the desired voltage vector at every sampling time. The X and Y coordinates of the intersection point can be found in (10) and (11), which demonstrate constant functions with representations of vertical and horizontal lines on the complex d-q plane, respectively. This finding implies that DB-DPQC can achieve independent P and Q control, which can be an evidence of exact nonlinear cross-coupling decoupling of the proposed control method.

If $\mathbf{e}_{sd,q}$ is aligned with the d-axis in every time instant, that is, $e_{sq} = 0$, then (10) corresponds to the difference between the current and next sample values of the reactive power ($\Delta q_{ins}(k)$). Similarly, the difference between the current and next sample values of the active power ($\Delta p_{ins}(k)$) is only represented by (11). Considering the graphical solution for the steady-state condition, in which $\Delta p_{ins}(k) = 0$ and $\Delta q_{ins}(k) = 0$ (no changes are observed in active and reactive power commands), is particularly intriguing, as shown in Fig. 3 with blue and red lines, respectively.

The drawn voltage vector provides a steady-state operation and constant DC link voltage such that it always lies on the q-axis from the origin to point "a", as shown by the green color vector. Active and reactive power changes in a single switching period are constrained by the hexagonal voltage limits. The power commands should be chosen to locate their intersection point inside the voltage limit to achieve DB-DPQC. Thus, (10) and (11) are directly solved to obtain the voltage vector required to compose the desired active and reactive powers over one switching period.

When $\Delta p_{ins}(k) > 0$, the line of the changes in active power moves downward to decrease the converter terminal voltage because additional power should be transferred from the grid

$$v_{tq}(k)T_s = -\frac{e_{sd}(k)}{e_{sq}(k)}v_{td}(k)T_s + \frac{1}{3e_{sq}(k)}\left(3T_s(e_{sq}^2(k)+e_{sd}^2(k)) - 2Lp_{ins}(k+1) + (2L-3RT_s)p_{ins}(k) - 3\omega LT_s q_{ins}(k)\right), \tag{8}$$

$$v_{tq}(k)T_s = \frac{e_{sq}(k)}{e_{sd}(k)}v_{td}(k)T_s + \frac{1}{3e_{sd}(k)}\left(2Lq(k+1) + (3RT_s - 2L)q(k) - 3\omega LT_s p(k)\right), \tag{9}$$

where $Y = v_{tq}(k)T_s$, $M' = -M^{-1} = \dfrac{e_{sq}(k)}{e_{sd}(k)}$, and $X = v_{td}(k)T_s$.

$$\begin{aligned} v_{td}(k)T_s = {} & \frac{e_{sd}(k)}{3(e_{sd}^2(k)+e_{sq}^2(k))}\left(3T_s(e_{sq}^2(k)+e_{sd}^2(k)) - 2Lp_{ins}(k+1) + (2L-3RT_s)p_{ins}(k) - 3\omega LT_s q_{ins}(k)\right) - \\ & \frac{e_{sq}(k)}{3(e_{sd}^2(k)+e_{sq}^2(k))}\left(2Lq_{ins}(k+1) + (3RT_s - 2L)q_{ins}(k) - 3\omega LT_s p_{ins}(k)\right), \end{aligned} \tag{10}$$

$$\begin{aligned} v_{tq}(k)T_s = {} & \frac{e_{sq}(k)}{3(e_{sd}^2(k)+e_{sq}^2(k))}\left(3T_s(e_{sq}^2(k)+e_{sd}^2(k)) - 2Lp_{ins}(k+1) + (2L-3RT_s)p_{ins}(k) - 3\omega LT_s q_{ins}(k)\right) + \\ & \frac{e_{sd}(k)}{3(e_{sd}^2(k)+e_{sq}^2(k))}\left(2Lq_{ins}(k+1) + (3RT_s - 2L)q_{ins}(k) - 3\omega LT_s p_{ins}(k).\right. \end{aligned} \tag{11}$$

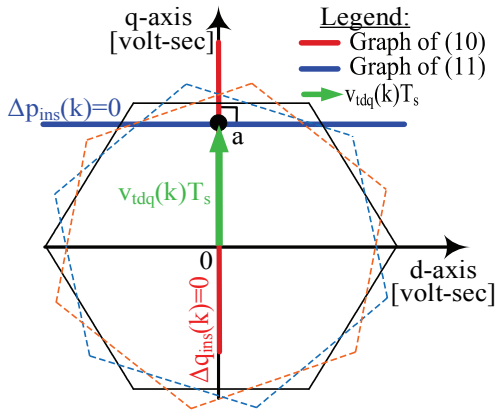

Fig. 3. Corresponding $\Delta p_{ins}(k)$ and $\Delta q_{ins}(k)$ power lines, their relevant voltage vectors, and the hexagon voltage limits on the d-q plane at steady-state condition.

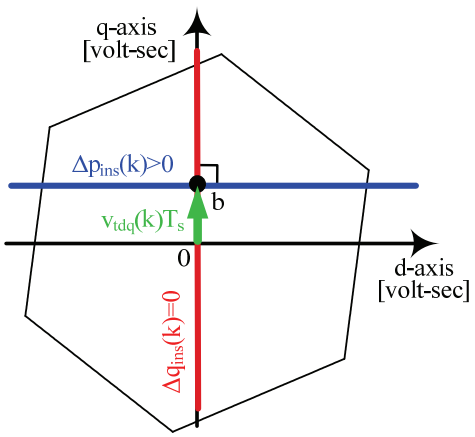

Fig. 4. DB-DPQC solution for active power command changes on the d-q plane under voltage limits.

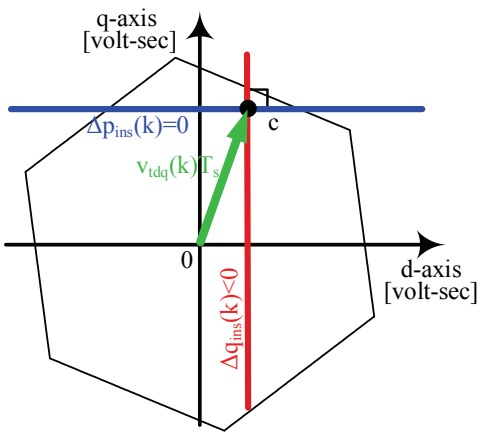

Fig. 5. DB-DPQC solution for reactive power command changes on the d-q plane under voltage limits.

to the load. Then, a new voltage vector at point "b" for the next sampling time is calculated to perform DB-DPQC, as shown in Fig. 4, where the active power can be independently controlled at the switching level.

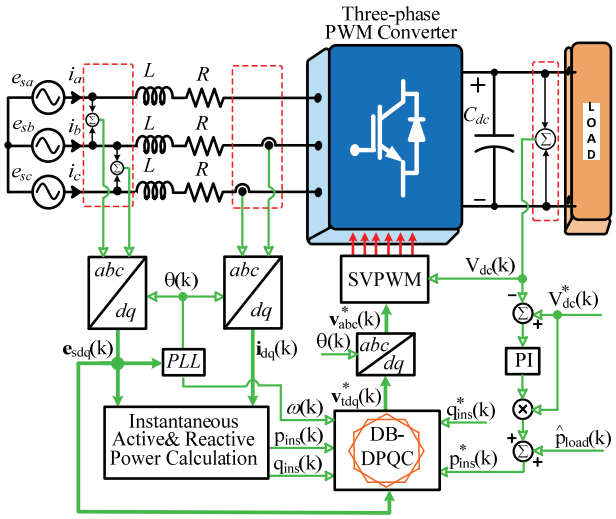

Fig. 6. Overall block diagram of the proposed DB-DPQC system.

Similar graphical solutions can be plotted for either reactive power or simultaneous active and reactive power commands with DB responses. When $\Delta q_{ins}(k) < 0$, the line of the changes in reactive power shifts to the right, and a new voltage vector is formed at point "c", as shown in Fig. 5.

Fig. 6 shows an overall block diagram of the control system with the proposed DB-DPQC algorithm in the discrete-time domain. The PI-type DC link voltage controller is implemented to regulate the DC link voltage, and the estimated load power $\hat{p}_{load}(k)$ is compensated for with a feedforward manner [16]. This structure leads to the DB direct power control law, which avoids the complexity of optimizing an additional switching table or cost functions.

Simple predictors are often utilized to compensate for computational delays when the DB control law is applied to power electronic converters. Given that the dynamics at the next sample instance can be estimated with a properly developed observer, the computation time delay can be compensated for by using this estimated value with the discrete-time current observer [17].

III. Evaluation via Simulation

An absolute time domain simulation of the proposed DPQC is conducted using a three-phase two-level AC/DC converter. A complete discrete-time control implementation is established in a MATLAB/Simulink environment to verify this analysis. The results are integrated into a co-simulation platform in Plecs® for the power electronics circuits. The system parameters used for this simulation are listed in Table I.

The first simulation evaluates the performance of the proposed controller to track the step changes in power commands. Fig. 7 shows p_{ins}, q_{ins}, $\mathbf{e}_{sabc}$, $\mathbf{i}_{sabc}$, V_{dc}, $|v^*_{td}|$, and $|v^*_{tq}|$ from top to bottom in the time domain profiles. The performance of the proposed DB-DPQC is independently

TABLE I
SYSTEM PARAMETERS

Parameter	Symbol	Value
Rated grid voltage (rms)	e_{sa}, e_{sb}, e_{sc}	220 $V_{rms,LL}$
Rated power	P_o	3 kW
Source frequency	f	60 Hz
DC link voltage	V_{dc}	350 V
DC link capacitor	C_{dc}	3300 μF
Boost inductance	L	1.8 mH
Sampling Time	T_s	100 μs

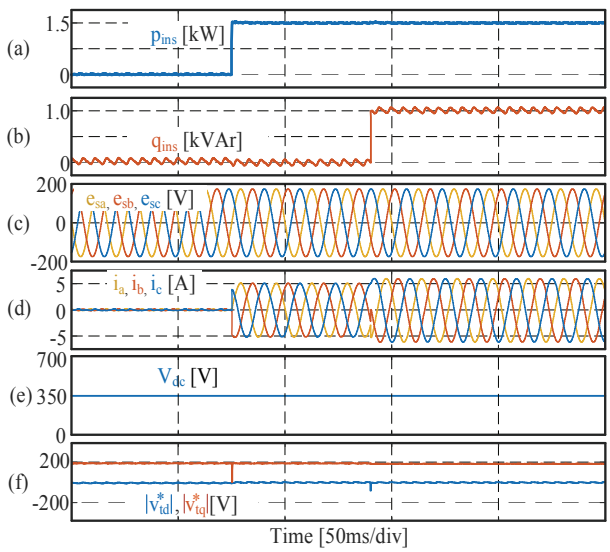

Fig. 7. Simulation results of converter operating with DB-DPQC presenting dynamic responses after step active and reactive power loadings.

examined for the step changes in p_{ins}, q_{ins}. Initially, the converter operates in a steady state with V_{dc} charged to 350 V and with no load conditions. Therefore, the magnitude of $|\mathbf{i}_{sabc}|$ remains at zero, and no average active or reactive power is applied. At t = 75 ms, p_{ins} is subjected to step change from 0 kW to 1.5 kW while q_{ins} is maintained to be constant at 0; at t = 140 ms, q_{ins} is changed from 0 kVAR to 1 kVAR while p_{ins} is maintained at 1.5 kW. Evidently, p_{ins} and q_{ins} rapidly follow their respective commands. The step changes of active and reactive power do not affect one another. This finding implies that the proposed DB-DPQC provides the exact cross-coupling decoupling. The phase currents are well regulated without any current control action.

Fig. 8 shows p_{ins}, p^*_{ins}, q_{ins}, q^*_{ins}, $|e_{sd}|$, $|e_{sq}|$, $|i_d|$, $|i_q|$, V_{dc}, $|v^*_{td}|$, and $|v^*_{tq}|$ from top to bottom. This test clearly shows that active power tracks the command in one sampling time. The q-axis converter output voltage command decreases when $\Delta p_{ins}(k) > 0$, as explained in Fig. 4. These voltage profiles imply that the desired vector solution lies within the hexagon, which is applied for a single T_s.

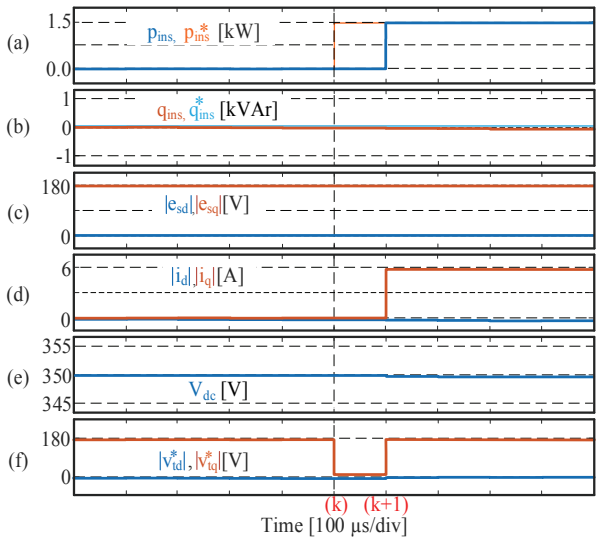

Fig. 8. DB response for active power command tracking.

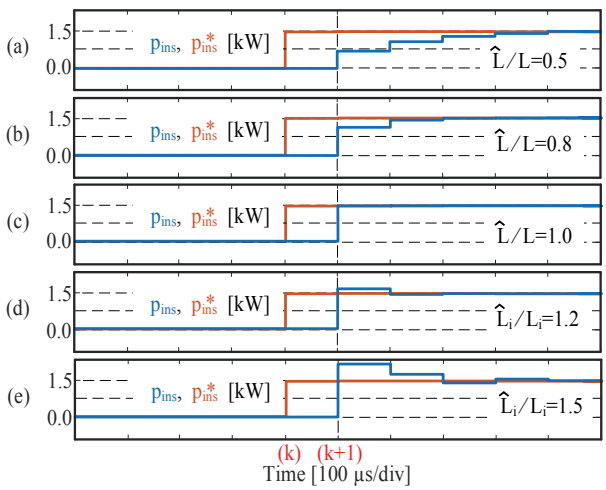

Fig. 9. Active power command tracking with the DB-DPQC under the inductor variations of: (a) −50%; (b) −20%; (c) 0%; (d) +20%; (e) +50%.

The proposed DB power regulation depends on the accuracy of the grid-side passive component values. The simulation results are presented in Fig. 9 for the DB-DPQC transient response under inductance variation conditions to evaluate the modeling error of the proposed controller. The modeling error causes a couple of multi-setting steps depending on the variation range. This test result indicates that the accurate and stable operation is sustained in the presence of parameter errors.

IV. EXPERIMENTAL RESULTS

A 3 kW laboratory-built PWM AC/DC converter is implemented to confirm the theoretical developments of the proposed algorithm. The running conditions in all experimental tests are identical to those in the simulation.

The dynamic responses to the stepped change in active and

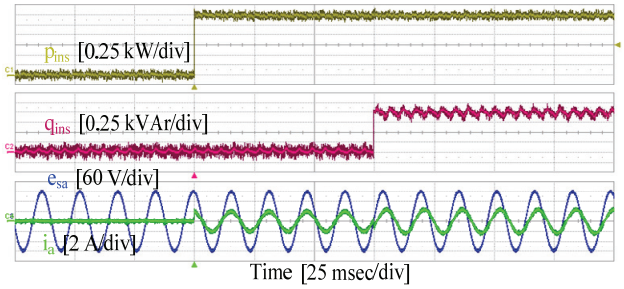

Fig. 10. Dynamic responses during active and reactive power step change.

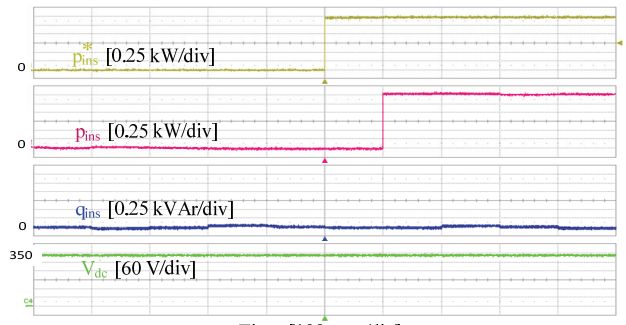

(a)

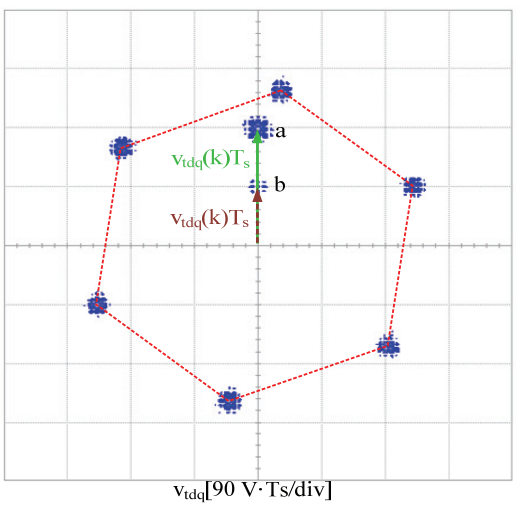

(b)

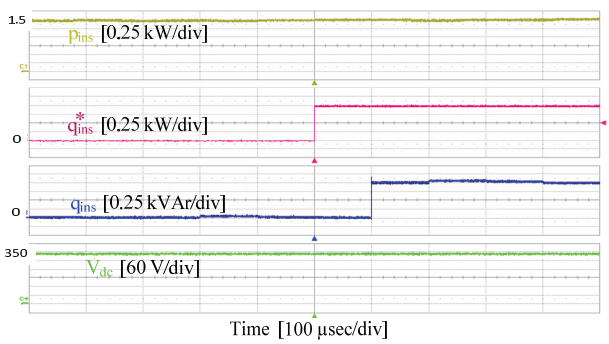

(c)

Fig. 11. DPQC response: (a) DB response of active power; (b) X-Y plot of the output voltage vector for active power command change; (c) DB response of reactive power.

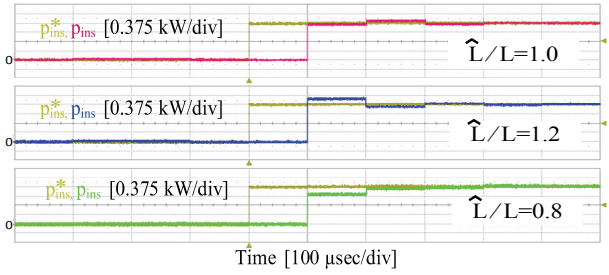

(a)

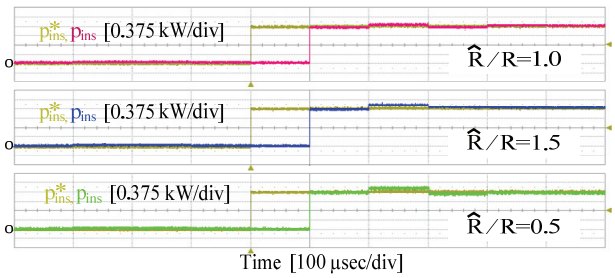

(b)

Fig. 12. Experimental results of active power command tracking with passive component variations for: (a) Inductance variations (±20%); (b) Resistance variations (±50%).

reactive powers are separately tested (Fig. 10). The active power, reactive power, and A-phase grid voltage/current are illustrated from top to bottom. The generated p_{ins} is almost constant and has no low-frequency oscillations; it is regulated at 1.5 kW. The sinusoidal input current without severe ripples and nearly united power factor is achieved under load conditions. At t = 150 ms, the reactive power is increased stepwise from 0% to 1 kVAR while the active power is still constant, resulting in non-unity power factor for per phase basis. The distortions of the active and reactive power are rarely found at the instant of the power step change because of the nature of cross-coupling decoupling.

Figs. 11(a) and (c) show a close-up view of the step change instant of the active and reactive powers. From top to bottom, active power command, controlled active power, reactive power, and measured DC link voltage are illustrated in Fig. 11(a). In Fig. 11(c), active power, reactive power command, controlled reactive power, and measured DC link voltage are illustrated. The DB dynamic response during the power step change is achieved with the response time of 100 µs (one sample time). The experimental results prove that the proposed DB control improves the dynamic performance and control accuracy without decreasing the control stability.

Fig. 11(b) illustrates the x-y plot of the output voltage when the active power command changes. As explained in Figs. 3 and 4, the voltage vector moves downward (from "a" to "b") to decrease the converter terminal voltage because additional power should be transferred from the grid to the load.

Fig. 12 shows the experimental results of the proposed method according to the passive parameter variations. The

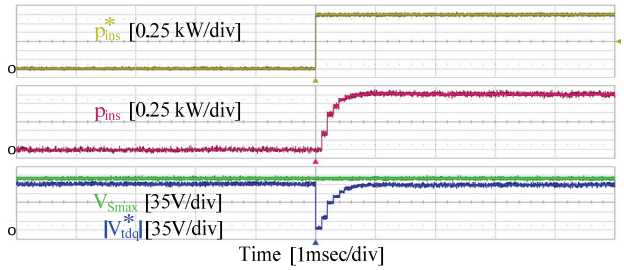

Fig. 13. Command tracking response of PI-type power controller.

active power responses are shown with the inductance and resistance variations. However, in practice, this condition may not be severe or even problematic because the values of R and L are easily measured or estimated with operating conditions.

As shown in Fig. 13, the dynamic control performance of the existing PI-type power controller [9] is compared to assess how the proposed DB-DPQC quickly tracks its command.

Active power command, controlled active power, maximum voltage (V_{Smax}), and output voltage magnitude ($|v^*_{tdq}|$) are illustrated from top to bottom.

For a fair comparison, the PI-type controller bandwidth is adjusted to utilize the nearly maximum available DC link voltage. At t = 5 ms, the output voltage magnitude moves downward to decrease the converter terminal voltage while its deviation reaches $V_{Smax,}$ which is around 200 V. This phenomenon implies that the PI power controller works under a nearly maximum control bandwidth and achieves the fastest tracking response at the given condition. When the identical step active power command used in the DPQC test in Fig. 11 (a) is applied, the tracking time reaches 10 times longer than that of the proposed DB-DPQC. This finding highlights that the proposed algorithm is promising for converter applications requiring fast operation.

V. Conclusions

In this paper, a fast DPQC is presented for three-phase PWM AC/DC converters used in newly emerging renewable applications. The proposed DB power controller guarantees the fastest transient response (one sample time). The principle is developed on the basis of the inverse model of the physical system to find the control voltage vector for tracking the active and reactive power commands. This choice of state variables allows an insightful graphical representation of the solution, including the voltage limits. The presented technique also provides DB control and cross-coupling decoupling between the active and reactive powers of the converter. The theoretical analysis is validated by the simulation and experimental results.

Acknowledgment

This work was supported by the 2016 Yeungnam University Research Grant.

References

[1] Y. Zhang, W. Xie, Z. Li and Y. Zhang, "Low-complexity model predictive power control: double-vector-based approach," *IEEE Trans. Ind. Electron*., Vol. 61, No. 11, pp. 5871-5880, Nov. 2014.

[2] E. Pouresmaeil, M. Mehrasa, and J. P. S. Catalao, "A multifunction control strategy for the stable operation of DG units in smart grids," *IEEE Trans. Smart Grid*, Vol. 6, No. 2, pp. 598-607, Mar. 2015.

[3] G. Kwon and Y. Suh. "Automatic command mode transition strategy of direct power control for PMSG MV offshore wind turbines," *Trans. Korea Inst. Power Electron.*, Vol. 21, No. 3, pp. 238-248, Jun. 2016.

[4] A. Yazdani and R. Iravani, *Voltage-sourced Converters in Power Systems: Modeling, Control, and Applications*, NewYork, NY, USA: Wiley-IEEE Press, 2010.

[5] Y. Cho and K. B. Lee, "Virtual-flux-based predictive direct power control of three-phase PWM rectifiers with fast dynamic response," *IEEE Trans. Power Electron*., Vol. 31, No. 4, pp. 3348-3359, Apr. 2016.

[6] D. O. Neacsu "Current control with fast transient for three-phase AC/DC boost converters," *IEEE Trans. Ind. Electron*., Vol. 51, No. 5, pp. 1117-1121, Oct. 2004.

[7] J. Q. N. Trinh, P. Wang and F. H. Choo, "An improved control strategy of three-phase PWM rectifiers under input voltage distortions and DC-offset measurement errors," *IEEE Trans. Emerg. Sel. Topics Power Electron*., Vol. 5, No. 3, pp. 1164-1176, Sep. 2017.

[8] J. Dannehl, C. Wessels, and F. W. Fuchs, "Limitations of voltage-oriented PI current control of grid-connected PWM rectifiers with LCL filters," *IEEE Trans. Ind. Electron*., Vol. 56, No. 2, pp. 380-388, Feb. 2009.

[9] M. Malinowski, M. Jasinski, and M. P. Kazmierkowski, "Simple direct power control of three-phase PWM rectifier using space-vector modulation (DPC-SVM)," *IEEE Trans. Ind. Electron*., Vol. 51, No. 2, pp. 447-454, Apr. 2004.

[10] S. J. Hong, C. B. Lee, H. S. Kim, J. H. Lee and C. Y. Won, "Feedforward compensation method of output voltage for improving dynamic characteristic of AC/DC PWM converter in DC distribution," in *Proc. IEEE ICEMS Conf*., pp. 1702-1708, 2015.

[11] Y. Zhang, Y. Peng, and C. Qu, "Model predictive control and direct power control for PWM rectifiers with active power ripple minimization," *IEEE Trans. Ind. Appl*., Vol. 52, No. 6, pp. 4909-4918, Nov./Dec. 2016.

[12] S Y. Zhang and C. Qu, "Model predictive direct power control of PWM rectifiers under unbalanced network conditions," *IEEE Trans. Ind. Electron*., Vol. 62, No. 7, pp. 4011-4022, Jul. 2015.

[13] C. Xia, M. Wang and Z. Song, and Tao Liu, "Robust model predictive current control of three-phase voltage source PWM rectifier with online disturbance observation," *IEEE Trans. Ind. Informat*., Vol. 8, No. 3, pp. 459-471, Aug. 2012.

[14] Y. Zhang, W. Xie, and Y. Zhang, "Deadbeat direct power control of three-phase pulse-width modulation rectifiers," *IET Power Electron.*, Vol. 7, No. 6, pp. 1340-1346, Jun. 2014.

[15] W. Jiang, X. Ding, Y. Ni, J. Wang, L. Wang, and W. Ma, "An improved deadbeat control for a three-phase three-line active power filter with current-tracking error compensation," *IEEE Trans. Power Electron*., Vol. 33, No. 3, pp. 2061-2072, Mar. 2018.

[16] S. K. Sul, *Control of Electric Machine Drive Systems*. NewYork, NY, USA: Wiley-IEEE Press, 2011.
[17] K. Lee, T. M. Jahns, T. A. Lipo, V. Blasko, and R. D. Lorenz, "Observer-based control methods for combined source-voltage harmonics and unbalance disturbances in PWM voltage-source converters," *IEEE Trans. Ind. Appl*., Vol. 45, No. 6, pp. 2010-2021, Nov./Dec. 2009.

Ali Gandomkar received his B.S. degree in Electronics and Electrical Engineering from Azad University, Tehran, Iran, in 2005; his M.S. degree in Industrial Electronics and Control from the University of Malaya, Kuala Lumpur, Malaysia, in 2012; and his Ph.D. in Control of Electrical Machinery and Power Conversion from the Department of Electrical Engineering, Yeungnam University, Gyeongsan, Korea, in 2017. He is working as a Postdoctoral Fellow in the Yeungnam University Power Conversion Laboratory. His current research interests include power electronics concerning DC/DC converters for renewable energy applications, power control of AC/DC/AC converters, and energy storage technologies.

Jul-Ki Seok received his B.S., M.S., and Ph.D. degrees in Electrical Engineering from Seoul National University, Seoul, Korea, in 1992, 1994, and 1998, respectively. Since 2001, he has been a member of the faculty of the School of Electrical Engineering, Yeungnam University, Gyeongsan, Korea, where he is currently a Professor. His specific research areas are motor drives, power converter control of offshore wind farms, and nonlinear system identification related to the power electronics field.